Cell Stress and Chaperones (2013) 18:503–516
DOI 10.1007/s12192-013-0406-2

ORIGINAL PAPER

A novel Omega-class glutathione *S*-transferase gene in *Apis cerana cerana*: molecular characterisation of *GSTO2* and its protective effects in oxidative stress

Yuanying Zhang · Huiru Yan · Wenjing Lu · Yuzhen Li · Xingqi Guo · Baohua Xu

Received: 2 December 2012 / Revised: 22 January 2013 / Accepted: 23 January 2013 / Published online: 6 February 2013

Abstract Oxidative stress may be the most significant threat to the survival of living organisms. Glutathione *S*-transferases (GSTs) serve as the primary defences against xenobiotic and peroxidative-induced oxidative damage. In contrast to other well-defined GST classes, the Omega-class members are poorly understood, particularly in insects. Here, we isolated and characterised the *GSTO2* gene from *Apis cerana cerana* (*AccGSTO2*). The predicted transcription factor binding sites in the *AccGSTO2* promoter suggested possible functions in early development and antioxidant defence. Real-time quantitative PCR (qPCR) and western blot analyses indicated that *AccGSTO2* was highly expressed in larvae and was predominantly localised to the brain tissue in adults. Moreover, *AccGSTO2* transcription was induced by various abiotic stresses. The purified recombinant *AccGSTO2* exhibited glutathione-dependent dehydroascorbate reductase and peroxidase activities. Furthermore, it could prevent DNA damage. In addition, *Escherichia coli* overexpressing *AccGSTO2* displayed resistance to long-term oxidative stress exposure in disc diffusion assays. Taken together, these results suggest that *AccGSTO2* plays a protective role in counteracting oxidative stress.

Keywords *Apis cerana cerana* · *GSTO2* · Gene expression pattern · Oxidative stress · Biochemical properties

Introduction

As normal by-products of oxygen metabolism, reactive oxygen species (ROS) are both harmful and beneficial to living systems (Valko et al. 2004). In low intracellular concentrations, ROS act as secondary messengers in signal transduction pathways regulating cell growth, while high ROS concentrations induce cellular senescence and apoptosis by oxidising nucleic acids, proteins, and lipids (Poli et al. 2004). In normal conditions, a dynamic balance between ROS generation and scavenging exists, resulting in a relatively low level of ROS maintained within cells. However, endogenous or exogenous insults can break this balance and lead to the excessive production or accumulation of ROS (i.e. oxidative stress). To defend against oxidative damage by ROS, organisms have evolved complex antioxidant defence systems to maintain normal cell structures and functions.

The glutathione *S*-transferases (GSTs, EC 2.5.1.18) family is a member of antioxidant defence systems that

Electronic supplementary material The online version of this article (doi:10.1007/s12192-013-0406-2) contains supplementary material, which is available to authorized users.

Y. Zhang · H. Yan · W. Lu · Y. Li · X. Guo (✉)
State Key Laboratory of Crop Biology College of Life Sciences, Shandong Agricultural University, Taian, Shandong 271018, People's Republic of China
e-mail: xqguo@sdau.edu.cn

B. Xu (✉)
College of Animal Science and Technology, Shandong Agricultural University, Taian, Shandong 271018, People's Republic of China
e-mail: bhxu@sdau.edu.cn

Y. Zhang
School of Basic Medical Sciences, Taishan Medical University, Taian, Shandong 271000, People's Republic of China

have dominant roles in regulating the intracellular ROS balance. GSTs catalyse the conjugation of reduced glutathione with compounds containing an electrophilic centre, which forms more soluble, nontoxic peptide derivatives that can be excreted from cells. Therefore, GSTs play central roles in the detoxification of endogenous and xenobiotic compounds, including drugs, herbicides and insecticides (Huang et al. 2011). GSTs also participate in the biosynthesis and intracellular transport of hormones and in the protection against oxidative stress (Hayes et al. 2005; Cnubben et al. 2001). GSTs are ubiquitous in both prokaryotes and eukaryotes. On the basis of insect GSTs sequence similarity, chromosomal location and immunological properties, insect cytosolic GSTs are currently divided into six classes, which are named Delta, Sigma, Epsilon, Zeta, Theta and Omega (Enayati et al. 2005).

The Omega-class GST (GSTO) was originally identified by analysing sequence similarities in the human expressed sequence tag (EST) database (Board et al. 2000). To date, GSTOs appear to be widespread in nature and have been identified in plants (Dixon et al. 2002), yeast (Garcera et al. 2006), insects (Walters et al. 2009), bacteria (Xun et al. 2010), and mammals (Rouimi et al. 2001). GSTOs have unique structural and functional characteristics. Within the canonical GST fold, GSTOs have a cysteine residue in their active site rather than the serine or tyrosine found in the other GST classes. Consequently, GSTOs catalyse a range of thiol transfer and reduction reactions that are rarely catalysed by members of the other classes (Board et al. 2000). Recently, GSTOs were shown to scavenge free radicals and ROS by modulating dehydroascorbate reduction and recycling (Rice 2000; Burmeister et al. 2008). GSTOs also participate in the biotransformation pathway of inorganic arsenic metabolism, which protects organisms from acute and chronic arsenic toxicosis (Chowdhury et al. 2006). There is increasing evidence that GSTOs are involved in various biological and clinically significant settings, including drug resistance (Yin et al. 2005), Alzheimer's disease (Li et al. 2003), the action of anti-inflammatory drugs (Laliberte et al. 2003), and susceptibility to chronic obstructive pulmonary disease (COPD) (Dulhunty et al. 2001). By regulating mitochondrial ATP synthase activity, DmGSTO1 has been demonstrated to play a protective role in a *Drosophila* model of Parkinson's disease (Kim et al. 2012). However, the role of GSTO in insect have not been fully investigated and should be further determined.

As a pollinator of flowering plants, *Apis cerana cerana* is a valuable indigenous species that plays an indispensable role in the balance of regional ecologies and agricultural economic development. Due to environmental deterioration in recent decades, farming this species is extremely difficult. The protective roles of GSTOs during oxidative stress have been invoked (Dixon et al. 2002; Kampkötter et al. 2003). To our knowledge, the molecular identity of hymenoptera GSTOs has not been investigated in comparison with other GST classes in hymenoptera species although the *Apis mellifera* genome was annotated. In this study, we isolated and characterised a *GSTO* gene, named *AccGSTO2*, from *A. cerana cerana*. In addition to assaying the biochemical properties of the purified *AccGSTO2*, we investigated the antioxidant ability of this protein. On the basis of these results, we infer that *AccGSTO2* might be one of the factors to perform functions in response to oxidative stress.

Materials and methods

Insects and treatments

A. cerana cerana worker bees were obtained from the experimental apiary of Technology Park of Shandong Agricultural University. The larvae and pupae were identified according to the criteria of Michelette and Soares (1993). The entire bodies of larvae, pupae and 1-day-old adult workers were collected from the hive. 10-day-old adult workers were obtained by marking newly emerged bees with paint and collecting them after 10 days. The brain, epidermis, flight muscle and midgut from adults (10d) were dissected on ice, frozen immediately in liquid nitrogen, and stored at −80 °C. Untreated larvae, pupae and adult workers were also frozen in liquid nitrogen and stored at −80 °C for analysis of developmental expression patterns. Moreover, the 10-day-old adults were fed on the basic adult diet containing water, 70 % powdered sugar and 30 % honey from the source colonies, and maintained in incubators at a constant temperature (34 °C) and humidity (70 %) under a 24 h dark regimen (Alaux et al. 2010). Then, they were divided into ten groups (n= 40/group). Groups 1–5 of adult workers were subjected to cold (4 °C, 16 °C, 25 °C), heat (42 °C), and ultraviolet (UV)-light (30 mJ/cm^2), respectively. Group 6 of adult workers were injected with 20 μl of H_2O_2 (50 μM of H_2O_2/worker) between the first and second abdominal segments using a sterile microscale needle. Considering that a bee in the wild is more likely to be exposed to insecticides through the cuticle when it lands on/rubs against a plant, groups 7–10 of adult workers for insecticide treatments, insecticides (cyhalothrin, phoxim, pyridaben, and paraquat) were delivered in 0.5 μl distilled water to the thoracic notum of worker bees and the final concentrations are 20 μg/L, 1 μg/mL, 10 μM, 10 μM, respectively. The adult workers were injected

with PBS as H_2O_2 controls in group 6. In insecticide treatments, adult workers were treated with 0.5-μl distilled water as controls. The adult workers were left untreated as controls in group 1–5. The adult workers of groups 1, 3, 7–10 were collected after treatment at 0.5, 1, 1.5, 2, and 2.5 h, while the groups 2, 4–6 at 1, 2, 3, 4, and 5 h. The treated bees were then immersed in liquid nitrogen and stored at −80 °C until used. These experiments were performed in triplicate.

RNA extraction, cDNA synthesis and DNA isolation

TRIzol reagent (Invitrogen, Carlsbad, CA, USA) was used to extract total RNA according to the manufacturer's protocol. Total RNA was digested with RNase-free DNase I to eliminate potential DNA contamination. First-strand cDNA was generated with the EasyScript First-Strand cDNA Synthesis SuperMix (TransGen Biotech, Beijing, China) according to the manufacturer's instructions. Genomic DNA was isolated using the EasyPure Genomic DNA Extraction Kit (TransGen Biotech, Beijing, China) according to the manufacturer's instructions.

Isolation of the cDNA, genomic sequence and the 5′-flanking region of *AccGSTO2*

To determine the cDNA and the genomic DNA sequences of *AccGSTO2*, cloning procedures were performed as previously described (Meng et al. 2011). The 5′-flanking region of *AccGSTO2* was amplified as previously described (Yu et al. 2011). The primer sequences used were provided in Supplementary Table 1. The MatInspector database (http://www.cbrc.jp/research/db/TFSEARCH.html) was used to predict putative *cis*-acting element and transcription factor binding sites in the 5′-flanking region of *AccGSTO2*. All of the PCR amplification conditions are shown in Supplementary Table 2.

Bioinformatic analyses

The conserved domains in AccGSTO2 were detected with the bioinformatics tools available at the NCBI server (http://blast.ncbi.nlm.nih.gov/Blast.cgi). Tertiary structures were predicted using SWISS-MODEL (http://swissmodelexpasy.org/). Using the DNAMAN software programme version 5.2.2, we identified the AccGSTO2 ORF and conducted multiple alignments of gene homologues. The Expasy-Sib Bioinformatics Resource Portal (http://web.expasy.org/compute_pi/) was used to predict the theoretical isoelectric point and molecular mass. The phylogenetic tree of the predicted amino acid sequences of GSTs from several insect species was constructed using the neighbour-joining method and the molecular evolution genetics analysis (MEGA) software programme, version 4.1.

Real-time quantitative PCR

cDNA synthesis was performed as described above. *β-actin* (XM640276) gene was selected as a reference gene to normalize qPCR experiments since it was validated among the most stably expressed genes tested in honey bee (Lourenco et al. 2008; Scharlaken et al. 2008). The *AccGSTO2* primer pairs RPF/RPR and *β-actin* primer pairs *β-actin-s*/*β-actin-x* were used for qPCR with the SYBR® PrimeScript™ RT-PCR Kit (TaKaRa, Dalian, China) in a CFX96TM Real-time System (Bio-Rad, Hercules, CA, USA). The qPCR programme was as follows: pre-denaturation at 95 °C for 30 s, 40 cycles of amplification (95 °C for 10 s, 55 °C for 20 s, and 72 °C for 15 s) and a melt cycle from 65 to 95 °C. mRNA abundance was evaluated in 3 independent biological replicates for each group with three technical repeats for each primer pair. The data were analysed with the CFX Manager software programme, version 1.1 using the $2^{-\Delta\Delta Ct}$ method (Livak and Schmittgen 2001).

Protein expression, purification and antibodies preparation

The expression of the recombinant AccGSTO2 was performed as previously described (Yu et al. 2011). The *AccGSTO2* coding region was ligated into pET-30a (+) vector (Novagen, Darmstadt, Germany) after digestion with the restriction endonucleases BamH I and Kpn I. The purification of target protein was performed with a method modified from Zhou et al. (2012). Briefly, the cells were centrifuged at 6,000×*g* at 4 °C for 10 min. The pellet was resuspended in 15 ml of lysis buffer (phosphate-buffered saline containing 15 % glycerol, 0.3 M NaCl and 20 mM imidazole, pH7.4), sonicated and centrifuged again at 4 °C (11,000×*g*, 15 min). Finally, both the supernatant and the pellet were solubilised in lysis buffer, and expression of the target recombinant protein was analysed by 12 % sodium dodecyl sulphate polyacrylamide gel electrophoresis (SDS-PAGE). The recombinant AccGSTO2 protein was purified on a HisTrap™ FF column (GE Healthcare, Uppsala, Sweden) according to the manufacturer's instructions. The supernatant was also loaded onto 1 ml of a HisTrap™ FF column equilibrated with lysis buffer for 1 h, and the protein was eluted with lysis buffer containing 0.25 M imidazole, pH7.4, and 0.5 M arginine to prevent precipitation and encourage refolding. The purified protein was examined by 12 % SDS-PAGE. The purified protein was injected subcutaneously into white mice for generation of antibodies as described by Meng et al. (2010).

Western blot analysis

Total protein from four different tissues (brain, epidermis, muscle, and midgut) and three different developmental stages (day-3 larvae, day-6 pupae, and day-10 adults) were extracted as described by Li et al. (2009). The total proteins were quantified with the BCA Protein Assay Kit (Thermo Scientific Pierce, IL, USA). Equal amounts of protein from four tissues or three developmental stages were subjected to 12 % SDS-PAGE and subsequently electrotransferred onto a polyvinylidene fluoride (PVDF) membrane (Millipore, Bedford, MA) using a Semi-dry Transfer Conit. Western blotting was performed according to the procedure of Meng et al. (2010). The anti-AccGSTO2 serum was used as the primary antibody at a 1:500 (*v*/*v*) dilution. Peroxidase-conjugated goat anti-mouse immunoglobulin G (Dingguo, Beijing, China) was used as the secondary antibody at a 1:2000 (*v*/*v*) dilution. The proteins were detected using the SuperSignal® West Pico Trial Kit (Thermo Scientific Pierce, IL, USA).

Enzymatic activity assays of recombinant AccGSTO2

Purified recombinant AccGSTO2 was dialysed in 100 mM KH_2PO_4, pH7.5, and used for the enzyme assays. The assays were performed in triplicate from three independent enzyme preparations. The 1-chloro-2,4-dinitrobenzene (CDNB)-conjugating activity was measured using spectrophotometry as described by Habig et al. (1974). Glutathione peroxidase activity was monitored using a method adapted from Boldyrev et al. (2001) in a reaction mixture containing 50 mM sodium phosphate buffer (pH7.8), 1 mM EDTA, 0.12 mM NADPH, 0.85 mM GSH as a substrate, 0.5 unit/ml glutathione reductase and 0.2 mM cumene hydroperoxide (or *t*-butylhydroperoxide). The reaction was initiated by adding the enzymatic extract, and it was recorded at 340 nm for 10 min at 25 °C. Glutathione-dependent dehydroascorbate reductase (DHAR) activity was measured by recording the increase in absorbance at 265 nm as described by Wells et al. (1995).

Optimum temperature and pH analysis

Because the recombinant AccGSTO2 showed detectable activity towards typical GST substrates, the effects of temperature and pH on enzymatic activity were determined by the standard DHAR assay. Enzyme activity for optimum temperature was determined by incubating the recombinant AccGSTO2 in the reaction mix contained of 200 mM sodium phosphate (pH6.85), 1 mM EDTA, 2.25 mM GSH and 1 mM DHA in a total volume of 1 ml. The reaction was initiated by adding DHA and recorded for 2 min over a temperature ranges from 5 to 55 °C in 5 °C increments with a 1-cm light path. Citrate buffer (50 mM, pH4.0–5.0), sodium phosphate buffer (50 mM, pH6.0–7.0) and Tris–HCl buffer (50 mM, pH8.0–9.0) were used to measure the optimal pH. All of the assays were performed in triplicate.

Kinetic parameter analysis

The DHAR apparent kinetic parameters of the recombinant GST were determined using a GSH range of 0.25-4.0 mM and a fixed DHA concentration of 1 mM; similarly, the apparent K_m and V_{max} values for DHA were determined using a DHA range from 0.1 to 2.0 mM and a fixed GSH concentration of 2.25 mM. All of the reactions were measured at pH6.85 and 25 °C. The apparent K_m and V_{max} values for CDNB (or GSH) were determined using a CDNB (or GSH) range from 0.1 to 4.0 mM and a fixed GSH (or CDNB) concentration of 1.0 mM. All of the reactions were measured at pH6.5 and 25 °C. The Michaelis constant was calculated using the Lineweaver–Burk method in the Hyper programme.

DNA cleavage assay with the MFO system

AccGSTO2 was characterised in a DNA protection assay modified from Yu et al. (2011). Briefly, a reaction mixture (25 μl) containing 100 mM HEPES buffer, 3 mM $FeCl_3$, 10 mM DTT, and increasing concentrations of AccGSTO2 protein ranging from 10 to 150 μg/ml was incubated at 37 °C for 30 min before the addition of 300 ng of pUC19 supercoiled plasmid DNA. The reaction was incubated for an additional 2.5 h at 37 °C and then subjected to 1 % agarose gel electrophoresis for the determination of DNA cleavage. *N*-ethylmaleimide (NEM, 5 mM) and BSA (150 μg/ml) were used as negative controls to add in this reaction mixture.

Disc diffusion assay under oxidative stress

Disc diffusion assay under oxidative stress was performed with a method modified from Burmeister et al. (2008). Briefly, approximately 5×10^8 bacterial cells were plated on LB-kanamycin agar plates and incubated at 37 °C for 1 h. Filter discs (6-mm diameter) soaked in different concentrations of cumene hydroperoxide (0, 25, 50, 80, or 100 mM), *t*-butylhydroperoxide (0, 2, 5, 8, or 10 mM), or paraquat (0, 10, 50, 100, or 200 mM) were placed on the surface of the top agar. The cells were grown for 24 h at 37 °C before the inhibition zones around the paper discs were measured.

Data analysis

Error bars denote standard error of the mean (SEM) from three independent experiments. The significant differences were determined by Duncan's multiple range tests using the Statistical Analysis System (SAS) version 9.1 software programmes (SAS Institute, Cary, NC, USA).

Results

Isolation and characterisation of *AccGSTO2* cDNA sequence

The sequence analysis indicated that the full-length cDNA of *AccGSTO2* (JX434029) was 1,365 bp, including a 321-bp 5′ untranslated region (UTR), a 324-bp 3′ UTR and a 720-bp complete ORF. The ORF encoded a polypeptide of 239 amino acids with a predicted molecular mass of 27.785 kDa and a theoretical isoelectric point of 6.21.

Multiple sequence alignments showed that AccGSTO2 shares 99.16–46.67 % sequence similarity to GSTO from *Apis florae* (AfGSTO1), *Bombus impatiens* (BiGSTO1), *Bombus terrestris* (BtGSTO1), *A. mellifera* (AmGSTO2), *Nasonia vitripennis* (NvGSTO2), *Harpegnathos saltator* (HsGSTO1), *Acromyrmex echinatior* (AeGSTO1), and *Camponotus floridanus* (CfGSTO1). In addition, the predicted AccGSTO2 contains the conserved features of the cytosolic GST superfamily, which include an N-terminal thioredoxin-like domain (H_5-D_{90}, with βαβαββα topology) and a C-terminal α-helixes domain (E_{102}–L_{225}). Moreover, the GSH-binding site (G-site) and putative substrate-binding site (H-site) were predicted using a bioinformatics tool on the NCBI server (Fig. 1a). This analysis indicated the AccGSTO2 belongs to the typical GSTOs (Board et al. 2000).

To determine the evolutionary relationships between AccGSTO2 and other insect GSTs, a neighbour-joining phylogenetic tree was built with 40 GSTs from different insects (Fig. 1b). Of the six classes insect GSTs examined, AccGSTO2 was categorised into the Omega class, where it clustered with AmGSTO2. Thus, we named the putative protein AccGSTO2.

To understand the relationships between the structure and function of AccGSTO2, its three-dimensional structure was predicted and reconstructed by SWISS-MODEL; the template that was used was the X-ray crystal structure of human Omega GSTO2-2 (PDB 3qagA), which was the second Omega GST structure determined. The two proteins share 30.67 % sequence identity. As shown in Fig. 1c, the N-terminal and C-terminal regions were located on the surface of the tertiary structure, and the overexpression of the pET-30a (+) vector did not affect the protein folding.

Identification of the genomic structure of *AccGSTO2*

To further elucidate the properties of *AccGSTO2*, the genomic DNA sequence of *AccGSTO2* was obtained by PCR amplification. The complete *AccGSTO2* (JX456219) is 2,147 bp, which includes six exons that are separated by five introns with high AT contents and canonical 5′-GT splice donor and 3′-AG splice acceptor sites. The *AccGSTO2* exons and introns were aligned with *GSTO* sequences from *A. cerana cerana*, *A. florea*, *B. impatiens*, *B. terrestris*, *and N. vitripennis* (Fig. 2). *AccGSTO2*, *AfGSTO1*, *BiGSTO1*, and *BtGSTO1* contained five introns and shared the highest length similarity, whereas *NvGSTO2* contained six introns. Moreover, because the first intron of *NvGSTO2* was located in the 5′ UTR, this gene was longer than the others.

Identification of partial putative *cis*-acting elements in the 5′-flanking region of *AccGSTO2*

To determine the organisation of the regulatory region of *AccGSTO2*, a 1,591-bp fragment (JX456219) located upstream of the transcription start site was isolated. Many *cis*-acting elements were predicted using the TFSEARCH software programme (Fig. 3). Sequences involved in tissue development and growth in early stages, including cell factor 2-II (CF2-II), Hunchback (Hb), Dfd, NIT2, Broad-Complex (BR-C), Pbx1, and caudal-related homeobox (CdxA) protein (Ericsson et al. 2006; Rørth 1994; Stanojević et al. 1989; Yu et al. 2011), were identified. In addition, several important transcription factors required for regulating various environmental stresses, such as heat shock factors (HSF) and activating protein-1 (AP-1), were predicted (Ding et al. 2005). The cAMP-responsive element binding protein (CREB) and the CCAAT/enhancer binding protein (C/EBP) were also found; and these elements regulate gene expression during cell differentiation, proliferation, and apoptosis (Ishida et al. 2007; Carlezon et al. 2005). We speculated that *AccGSTO2* may be involved in organismal development and environmental stress responses.

Temporal and spatial expression patterns of *AccGSTO2*

QPCR was performed to examine the expression patterns of *AccGSTO2* during different developmental stages. As shown in Fig. 4a, the expression level of *AccGSTO2* gradually decreased from the day-3 larvae to the day-1 adults, and increased rapidly in day-10 adults. The highest expression level was detected in day-3 larvae, and almost no significant

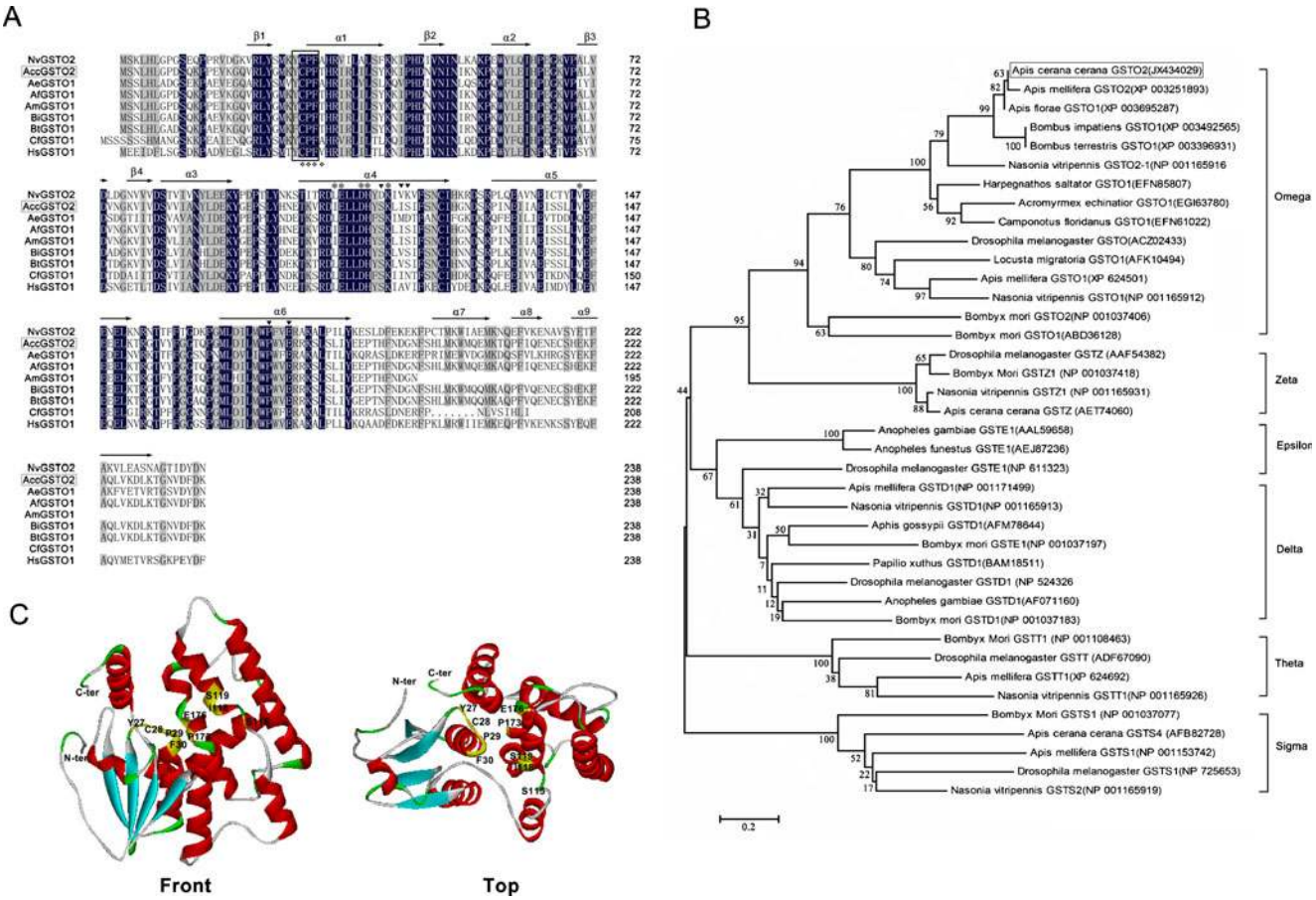

Fig. 1 Molecular properties of AccGSTO2. **a** The amino acid sequence alignment of AccGSTO2 and other GSTOs. The putative secondary structure of AccGSTO2 is shown. Identical amino acids are *shaded in black*. The conserved functional domains are boxed. The putative G-site, H-site and dimer interface of AccGSTO2 are denoted by (❖), (*inverted filled triangle*) and (❄), respectively. **b** Phylogenetic relationships between glutathione transferases (GSTs) from different insect species. The six primary classes are shown, and AccGSTO2 is boxed. **c** The tertiary structure of AccGSTO2. The conserved G-site residues (Y27, C28, P29, and F30), H-site residues (S115, I118, S119, P173, and E176), N-terminal, and C-terminal are shown

differences in *AccGSTO2* expression were observed during pupae stages.

Among the adult tissues studied, the most pronounced expression appeared in the brain, and decreasing mRNA levels

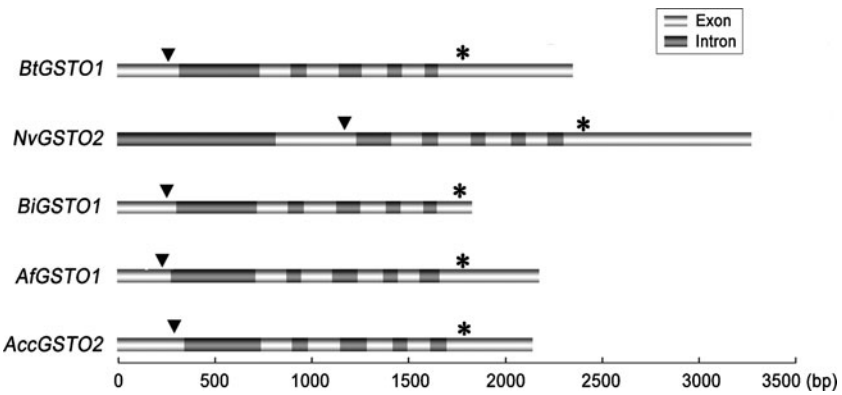

Fig. 2 Genomic structure of the Omega-class glutathione transferase genes (*GSTOs*). The lengths of the exons and introns of genomic DNA from *A. cerana cerana*, *A. florea*, *B. impatiens*, *B. terrestris*, *and N. vitripennis* are shown according to the scale below. Light grey and grey are used to highlighted the exons and introns separately. The translational initiation codons (ATG) and termination codons (TAA) are marked by (*inverted filled triangle*) and (*asterisk*), respectively

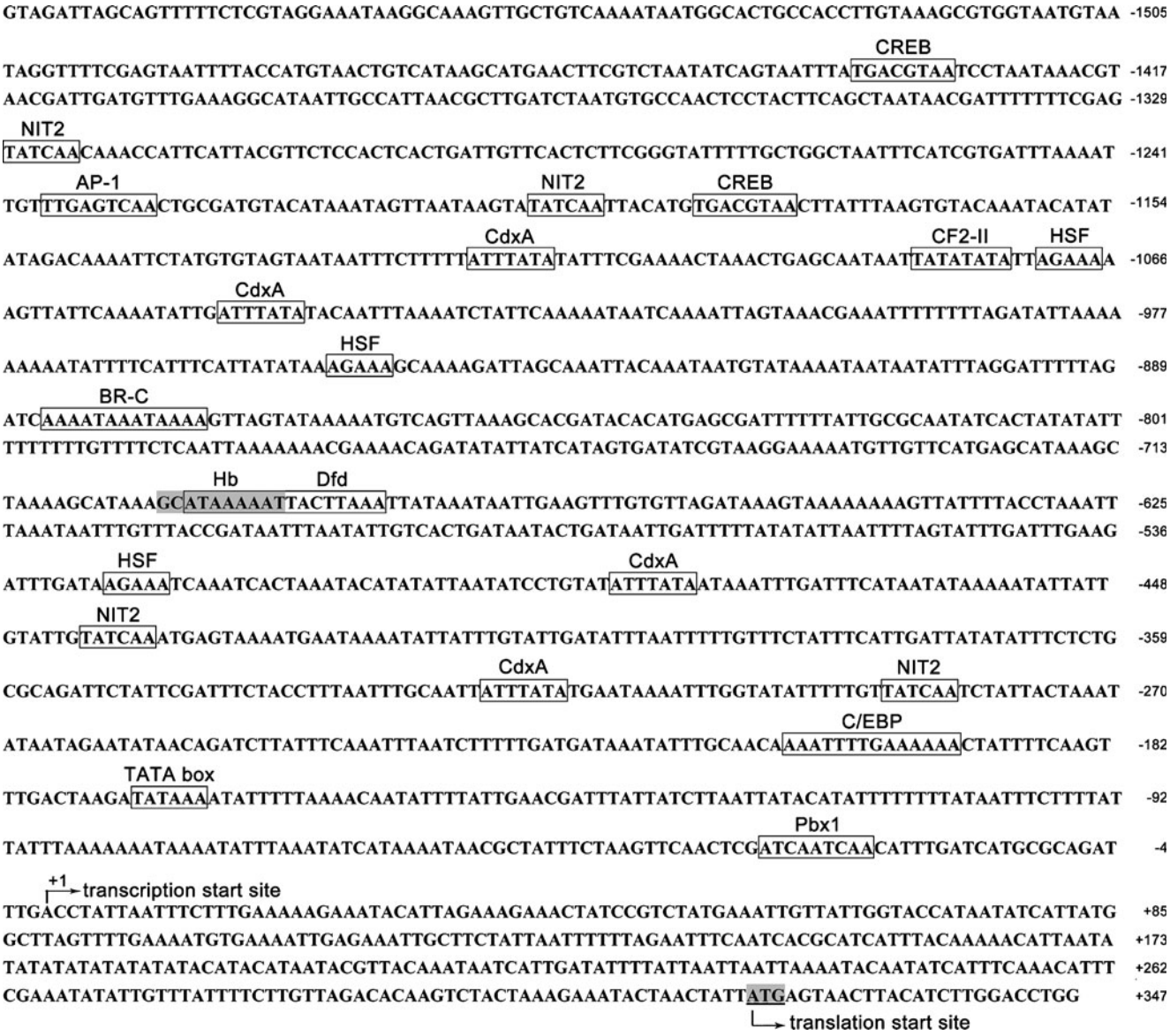

Fig. 3 The nucleotide sequence and putative *cis*-acting elements of the *AccGSTO2* regulatory region. The translation and transcription start sites are marked with arrows. The *cis*-acting elements are *boxed*, with the exception of Hb, which is *shaded in black*

of *AccGSTO2* were observed in the epidermis, muscle and midgut (Fig. 4b). The brain is a highly sensitive tissue for xenobiotics and peroxidative damage, implying that *AccGSTO2* may play a protective role in the brain tissue.

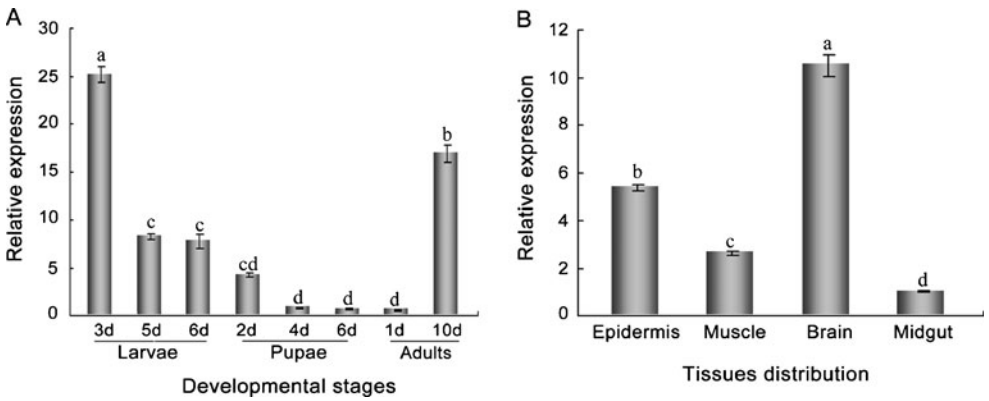

Fig. 4 Expression profile of *AccGSTO2* as determined by qPCR. The relative expression of *AccGSTO2* at different developmental stages (**a**) and in different tissues (**b**) is shown. The data are the means±SE of three independent experiments. The *different letters above the columns* indicate significant differences ($P<0.01$) according to Duncan's multiple range tests

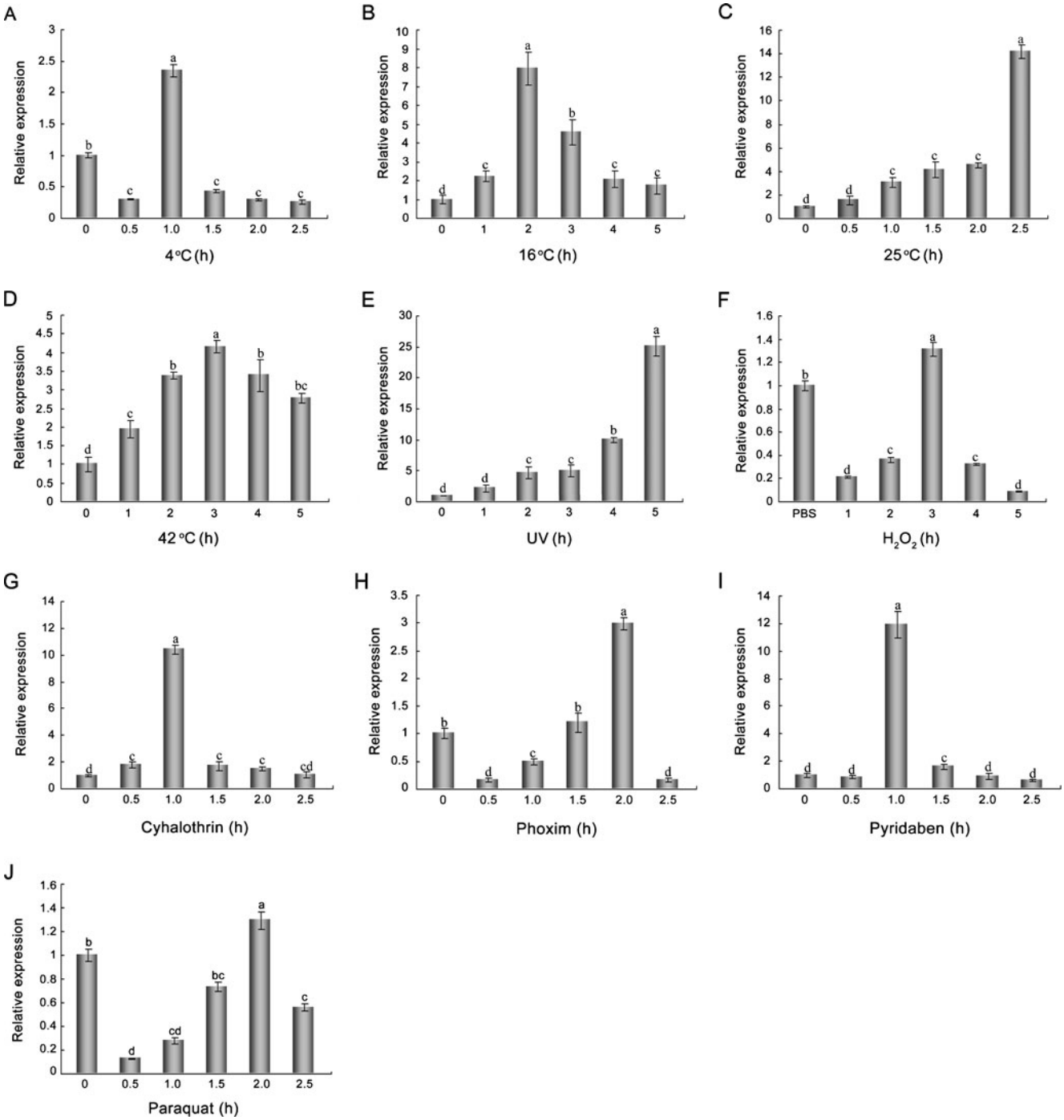

Fig. 5 Expression profile of *AccGSTO2* under different stress conditions. These conditions included 4 °C (**a**), 16 °C (**b**), 25 °C (**c**), 42 °C (**d**), UV (30mj/cm^2) (**e**), H_2O_2 (2 mM) (**f**), Cyhalothrin (20 μg/l) (**g**), Phoxim (1 μg/ml) (**h**), Pyridaben (10 μM) (**i**), and Paraquat (10 μM) (**j**). Untreated adult worker bees (*Lane 0*) were used as controls, and adult worker bees injected with PBS for 5 h were used as injection controls. The data are the means±SE of three independent experiments. The *different letters above the columns* indicate significant differences ($P<0.01$) according to Duncan's multiple range tests

Expression patterns of *AccGSTO2* under abiotic stress treatments

Knowledge on the expression patterns of *AccGSTO2* under environmental stressors could be helpful to better understands the biological functions. Previous studies have indicated that the expression of *GSTO* could be induced by environmental stressors such as heat, heavy metals and endocrine-disrupting chemical in disk abalone (Wan et al. 2009), insecticides and UV radiation in the silkmoth (Yamamoto et al. 2011). To

determine whether *AccGSTO2* is involved in different abiotic stress response, relative expressions of *AccGSTO2* under temperature (4, 16, 25, 42 °C), UV, H_2O_2 and insecticide (cyhalothrin, phoxim, pyridaben, paraquat) exposure were detected by qPCR. As shown in Fig. 5, *AccGSTO2* expression was up-regulated under all treatments tested, although there were different expression patterns and increased degrees. These results indicate that *AccGSTO2* may be involved in abiotic stress responses.

Western blot analysis

To further verify the temporal and spatial expression patterns of *AccGSTO2*, total protein was detected from four different tissues (epidermis, muscle, brain and midgut) of the day-10 adults or three different developmental stages (day-3 larvae, day-6 pupae, and day-10 adults) and probed with anti-*AccGSTO2* serum (Fig. 6). The expression of *AccGSTO2* was consistent with its transcript expression in different tissues or developmental stages.

Purification and enzymatic features of recombinant AccGSTO2 protein

To further characterise the recombinant AccGSTO2 protein, the complete *AccGSTO2* ORF lacking a stop codon was cloned into the pET-30a (+) vector, and it was expressed in *E. coli* BL21 (DE3) as a histidine-fusion protein via IPTG induction. A sodium dodecyl sulphate polyacrylamide gel electrophoresis (SDS-PAGE) analysis showed that the recombinant protein was soluble and had a molecular mass of approximately 34 kDa, which is consistent with the predicted molecular mass of 34.804 kDa (Fig. 7). The soluble recombinant protein was further purified by HisTrap™ FF columns, and the concentration of the purified AccGSTO2 was approximately 1.89 mg/ml.

To identify the catalytic activities and potential biological functions of AccGSTO2, its substrate specificity with several typical GST substrates was determined. The purified enzyme showed detectable GSH-conjugating activity towards CDNB (the K_m and V_{max} values for CDNB were 2.32±0.25 mM and 8.21±1.67 μmol/min per mg protein, respectively, and the K_m and V_{max} values for GSH were 1.14±0.16 mM and 9.77±0.11 μmol/min per mg protein, respectively) and measurable GSH peroxidase activity towards cumene hydroperoxide (V_{max}=3.24±0.23 μmol/min per mg protein) and *t*-butylhydroperoxide (V_{max}=1.17±0.28 μmol/min per mg protein). Moreover, AccGSTO2 could use GSH as an electron donor to reduce dehydroascorbate (the K_m and V_{max} values for DHA were 0.46±0.09 mM and 8.11±1.56 μmol/min per mg protein, respectively, and the K_m and V_{max} values for GSH were 3.55±0.73 mM and 6.35±1.37 μmol/min per mg protein, respectively), exhibiting high-affinity specificity towards DHA. Furthermore, the recombinant AccGSTO2 showed a maximum DHAR activity at pH 7.0 and an optimum temperature of 25 °C (Fig. 8).

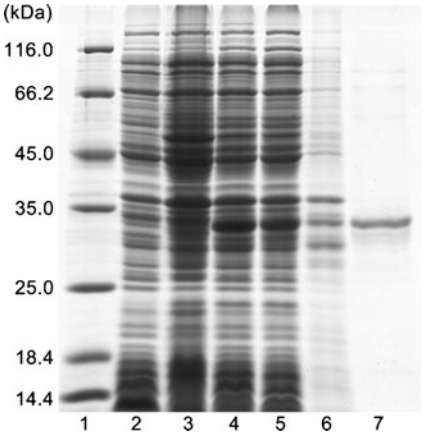

Fig. 7 Expression and purification of AccGSTO2. An SDS-PAGE analysis was used to separate recombinant AccGSTO2 expressed in *E. coli* BL21 cells. *Lane 1* low molecular weight protein marker; *Lane 2* induced overexpression of pET-30a (+) in BL21. *Lanes 3 and 4* non-induced and induced overexpression of pET-30a (+) -AccGSTO2 in BL21, respectively; *Lanes 5 and 6* suspension and pellet of sonicated recombinant AccGSTO2, respectively; *Lane 7* purified recombinant AccGSTO2

Protective effects of recombinant AccGSTO2 protein in oxidative stress

To provide a direct evidence that AccGSTO2 is responsible for antioxidant defence, the mixed-function

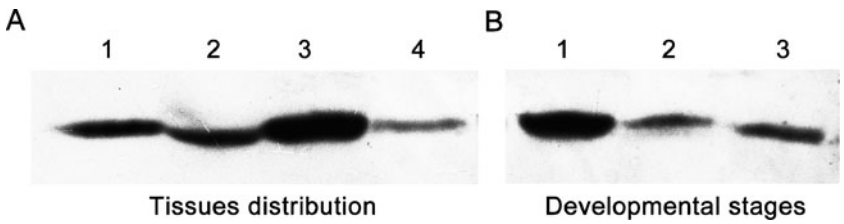

Fig. 6 Western blot analysis of AccGSTO2 in different tissues and developmental stages. **a** *Lanes 1–4* were loaded with an equivalent amount of protein: *Lane 1* epidermis, *Lane 2* muscle, *Lane 3* brain, *Lane 4* midgut. **b** *Lanes 1–3* were loaded with an equivalent amount of protein: *Lane 1* day-3 larvae, *Lane 2* day-6 pupae, and *Lane 3* day-10 adults

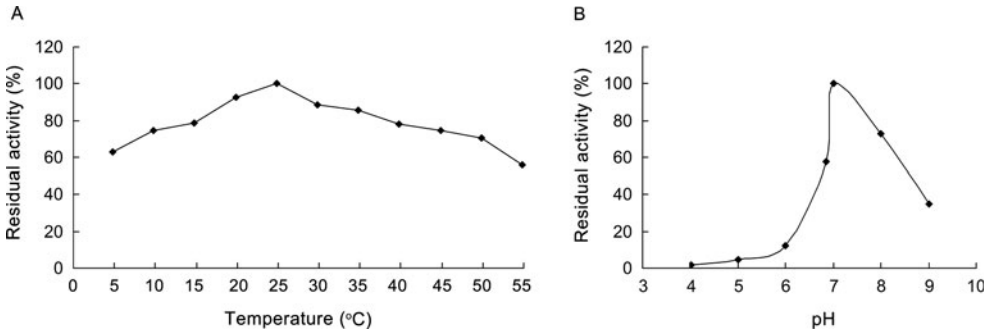

Fig. 8 Temperature (**a**) and pH (**b**) effects on the catalytic activity of AccGSTO2. The DHAR activities of recombinant AccGSTO2 were tested at different temperatures (5–55 °C) and pH values (4.0–9.0). The values are the means of three replicates

oxidation (MFO) system, which produces hydroxyl radicals, was chosen to test whether AccGSTO2 protects DNA from ROS damage (Yu et al. 2011). As shown in Fig. 9, with increasing concentrations of recombinant AccGSTO2, the amount of the nicked form of the plasmid declined gradually. When the concentration of AccGSTO2 was 150 μg/ml, the nicked form was nearly undetectable. *N*-ethylmaleimide (NEM) contains a reactive double bond and is used to modify cysteine residues. When added to the MFO reaction, NEM inhibited the AccGSTO2 protection of DNA. Therefore, we concluded that the sulfhydryl moieties of cysteine residues in AccGSTO2 may play important roles in DNA protection.

Disc diffusion assay provides a further evidence for its protective effects in oxidative stress. After exposed overnight to various stressors, the killing zones around the drug-soaked filters were smaller on the plates containing *E. coli* overexpressing *AccGSTO2* than in the control bacteria; 21 % (cumene hydroperoxide), 31 % (*t*-butylhydroperoxide), and 31 % (paraquat) halo reductions were observed (Fig. 10). The model external prooxidants cumene hydroperoxide and *t*-butylhydroperoxide were used because they are more stable than H_2O_2 under the applied incubation conditions. Because paraquat are redox-active and can cross cell membranes, they were used as intracellular ROS inducers to generate superoxide anions from molecular oxygen during metabolism (Burmeister et al. 2008).

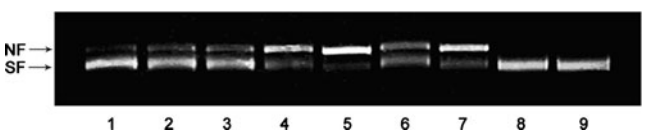

Fig. 9 *AccGSTO2* protected DNA from oxidative damage in the mixed-function oxidation system. *Lanes 1–4* pUC19 plasmid DNA+$FeCl_3$+DTT+purified AccGSTO2 (150, 100, 50 and 10 μg/ml, respectively); *Lane 5* pUC19 plasmid DNA+$FeCl_3$+DTT; *Lane 6* pUC19 plasmid DNA+$FeCl_3$+DTT+purified AccGSTO2 (50 μg/ml)+NEM (5 mM); *Lane 7* pUC19 plasmid DNA+$FeCl_3$+DTT+BSA (150 μg/ml); *Lane 8* pUC19 plasmid DNA+$FeCl_3$; *Lane 9* pUC19 plasmid DNA only. *SF* supercoiled form; *NF* nicked form

Discussion

The GSTOs play central roles in detoxifying endogenous and exogenous agents. This gene family is particularly interesting because it is involved in human disease and exists in a wide range of species (Board 2011). However, research concerning GSTOs has mainly focused on mammals, and there is limited information on GSTO in insects (Ketterman et al. 2011). In this study, we described the cloning and characterisation of a novel GSTO from *A. cerana cerana*. Unlike most GSTOs, the recombinant AccGSTO2 had DHAR activity and GSH-dependent peroxidase activity, and it also catalysed the conjugation of CDNB. These results were consistent with two recent studies by Burmeister et al. (2008) and Garcera et al. (2006). The precise mechanism involved in the distinct enzymatic features has not yet been elucidated. Wan et al. (2009) postulated that a non-traditional GST active site contributed to these differences in activity. The compositions of the cysteine-containing tetramers are as divergent as F-C-P-Y, F-C-P-F, F-C-P-W, Y-C-P-F, Y-C-P-Y, etc. AccGSTO2 was unique because its tetramer sequence was Y-C-P-F; unlike most GSTOs, tyrosine (Y) replaced phenylalanine (F) in the first residue. This substitution likely reflects a stronger interaction between the hydroxyl groups of the tyrosine and glutathione molecules. Although this explanation hints at distinct enzymatic features for different GSTOs, it remains to be tested experimentally.

The 5′-flanking region of *AccGSTO2* contains many predicted transcription factor binding sites involved in early development. To confirm whether *AccGSTO2* is involved in early development, we performed a stage-specific expression analysis of *AccGSTO2*. The qPCR analyses indicated that *AccGSTO2* is highly expressed in larvae stage (Fig. 4a). Krishnan and Sehnal (2006) reported that larvae and adults suffer higher oxidative stress than pupae because during the larval stages and the first two weeks of adulthood, their diet is restricted to honey, pollen and glandular secretions provided by other colony members. Because the pupal stages and first instar adults are at a quiescent non-feeding stage, the active intake and digestion of foods that either contain or

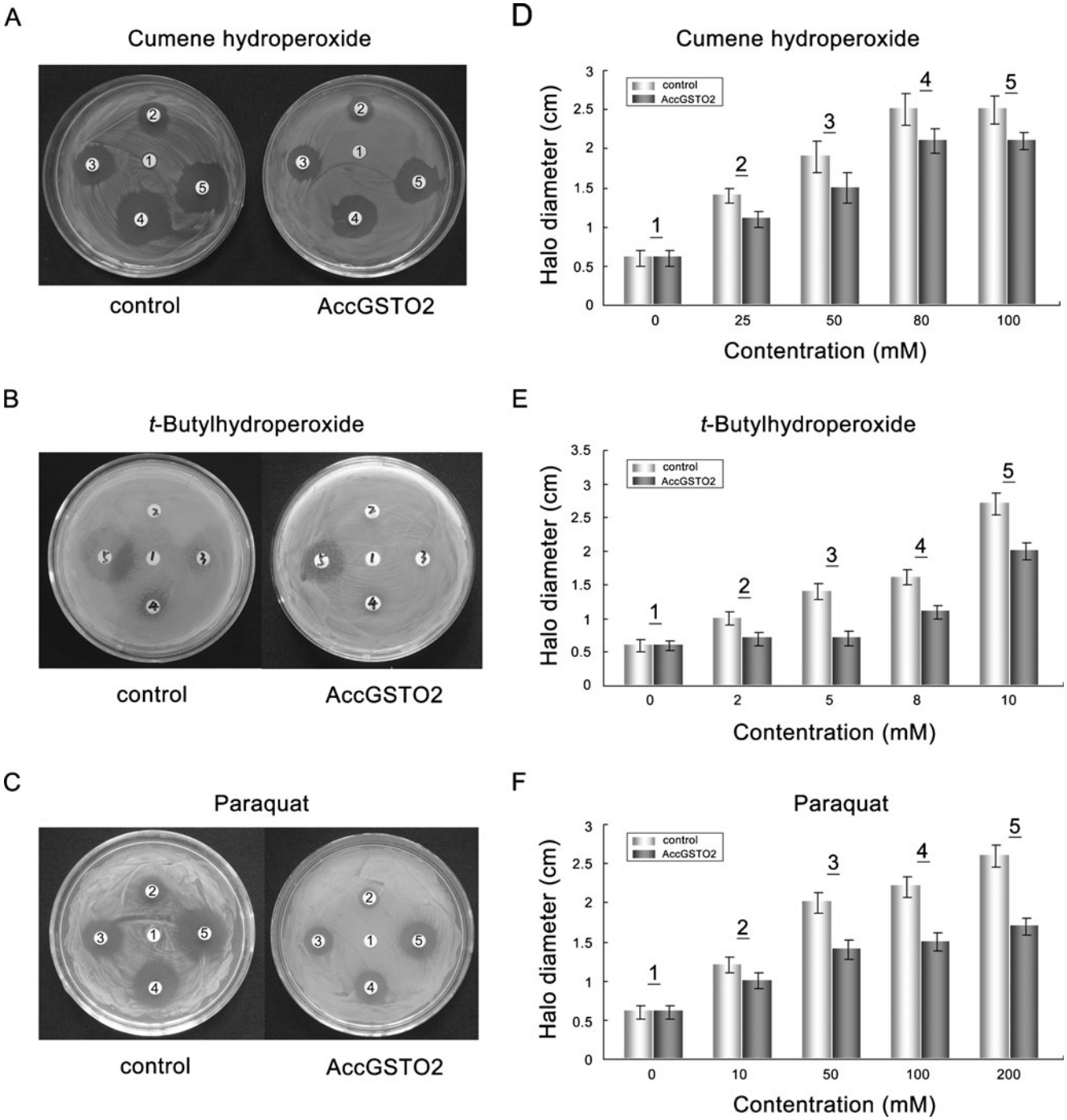

Fig. 10 Disc diffusion assays using *E. coli* overexpressing *AccGSTO2*. LB agar plates were inoculated with 5×10^8 cells. *AccGSTO2* was overexpressed in *E. coli* and bacteria transfected with pET-30a (+) were used as negative controls. Filter discs soaked with different concentrations of cumene hydroperoxide (**a**, **d**), *t*-butylhydroperoxide (**b**, **e**) or paraquat (**c**, **f**) were placed on the agar plates. After an overnight exposure, the killing zones around the drug-soaked filters were measured

produce potentially toxic oxidative radicals may cause higher oxidative stress levels in the larval and adult stages. Moreover, microsomal oxidases have been shown to be active in honeybee larvae (Gilbert and Wilkinson 1975). An incomplete antioxident or immune defence system in larvae may explain this pattern because they are more susceptible to environmental stresses. Thus, the higher transcriptional levels of *AccGSTO2* in larvae stage suggest a potential role in the detoxification of xenobiotics in their food in early development.

Knowledge on the tissue distributions of *AccGSTO2* mRNA could be helpful to better understands the physiology.

A tissue-specific expression analysis revealed that *AccGSTO2* mRNA was expressed at its highest levels in the brain (Fig. 4b), which is very sensitive to oxidative stress (Ament et al. 2008; Rival et al. 2004). This observation is inconsistent with the low expression of *GSTO* in the mammalian brain (Board et al. 2000). However, CG6781/se from *Drosophila melanogaster* was only found in significant levels in brain regions involved in pteridine metabolism and the biosynthesis of red eye pigments (Walters et al. 2009). Furthermore, we found that AccGSTO2 had significant DHAR activity. This activity may be critical for maintaining ascorbic acid (AsA) levels in the brain because AsA is dependent on the uptake and subsequent enzymatic reduction of DHA. AsA plays a major role in scavenging free radicals and specific ROS (Frei et al. 1989), and due to the significant consumption of oxygen in the brain, the scavenging and detoxification of these reactive species is imperative. Taken together, the abundant expression of *AccGSTO2* in the brain tissue implied that it may play important roles in protection against oxidative stress by maintaining AsA levels.

Studies on the insect GSTs mainly focused on their roles in insecticide resistance (Enayati et al. 2005) and oxidative stress responses (Corona and Robinson 2006; Li et al. 2008). The various insect GSTs play protective roles through different defence mechanisms. The insect-specific Delta-class and Epsilon-class GSTs are thought to be major contributors to detoxification and insecticide resistance (Ketterman et al. 2011). In addition, some Epsilon-class GSTs in mosquito have peroxidase activity and may be important in protection against oxidative stress (Lumjuan et al. 2005; Ortelli et al. 2003). The insect Sigma-class and Theta-class GSTs are implicated in the detoxification of lipid peroxidation products, suggesting a protective role against oxidative stress (Singh et al. 2001; Yamamoto et al. 2005). The Zeta-class GSTs may have common housekeeping functions in the tyrosine degradation pathway, including cellular defence against oxidative stress (Claudianos et al. 2006). For the Omega-class GSTs, this protective role against oxidative stress is mediated by DHA reductase and thiol transferase activities (Yamamoto et al. 2011), whereas other insect GSTs do not exhibit these activities. Currently, lack of knowledge of endogenous insect GST substrates makes it difficult to elucidate the precise roles of different insect GST classes, and not all insect GSTs are involved in detoxification and antioxidative stress (Huang et al., 2011). In this study, several antioxidant response elements, such as HSF and AP-1, were predicted in the 5′-flanking region of *AccGSTO2*. Furthermore, the qPCR analysis revealed that *AccGSTO2* was induced by all abiotic stressors examined, such as temperature, H_2O_2, insecticides and UV radiation can induce oxidative stress (Lushchak 2011; Kottuparambil et al. 2012). Consistent with these results, *GSTO* from *Bombyx mori* is activated by a variety of environmental stimuli, including bacteria, ultraviolet-B (UV-B) and three commonly used chemical insecticides (Yamamoto et al. 2011). These results suggest that the function of GSTOs in insects is conserved. In general, the elevated mRNA levels of *GSTO* are always correlated with their known roles (Huang et al. 2011; Yamamoto et al. 2011; Wan et al. 2009). This appears to the case in *C. elegans*, where specific silencing of the GSTO1-1 by RNAi created worms with an increased sensitivity to several pro-oxidants, arsenite, and heat shock (Burmeister et al. 2008). This observation provides clue for the role of *AccGSTO2* in the defence response. Therefore, an increase in amount of *AccGSTO2* expression under various abiotic stressors may be related to increased tolerance of oxidative stress; however, it should be further explored.

GSH-dependent peroxidase is a well-known enzyme that functions as an antioxidant by reducing organic hydroperoxides to the less toxic monohydroxy alcohols and protecting the lipid membranes and other cellular components against oxidative stress (Mahmoud and Edens 2003). However, the lack of Se-dependent glutathione peroxidases in insects increases the potential importance of the putative Se-independent peroxidase function of GSTs in antioxidant defence (Corona and Robinson 2006). DHAR activity may maintain AsA levels, which plays a major role in scavenging free radicals and specific ROS (Frei et al. 1989). Yamamoto et al. (2011) also demonstrated that bmGSTO plays a role in scavenging ROS by peroxidase activity and induces resistance to oxidative stress by DHAR activities. In our study, *AccGSTO2* exhibited glutathione-dependent DHAR and peroxidase activities. Moreover, the transcription of *AccGSTO2* is induced by H_2O_2 and paraquat treatment. The disc diffusion assay also provides direct evidence that *E. coli* cells overexpressing *AccGSTO2* were protected from environmental stressors (paraquat, cumene hydroperoxide, and *t*-butylhydroperoxide). In addition, the recombinant AccGSTO2 can protect supercoiled DNA from nicking by hydroxyl radicals in the MFO system. Taken together, these observations indicate that *AccGSTO2* could be associated with the scavenging of ROS and contribute to the cells resistance to oxidative stress.

Protection against oxidative stress is an eternal theme for the survival of living organisms. In conclusion, the unique biochemical features, expression patterns, functional characteristics and potential physiological roles of *AccGSTO2* that were demonstrated in this study offer the basic knowledge for further studies about functions of Omega-class GST.

Acknowledgments This work was financially supported by the National Natural Science Foundation (No. 31172275) in China, the Agroscientific Research in the Public Interest (No. 200903006) and the China Agriculture Research System (No. CARS-45).

References

Alaux C, Ducloz F, Crauser D, Le Conte Y (2010) Diet effects on honeybee immunocompetence. Biol Lett 6:562–565

Ament SA, Corona M, Pollock HS, Robinson GE (2008) Insulin signaling is involved in the regulation of worker division of labor in honey bee colonies. Proc Natl Acad Sci USA 105:4226–4231

Board PG, Coggan M, Chelvanayagam G, Easteal S, Jermiin LS, Schulte GK, Danley DE, Hoth LR, Griffor MC, Kamath AV, Rosner MH, Chrunyk BA, Perregaux DE, Gabel CA, Geoghegan KF, Pandit J (2000) Identification, characterization, and crystal structure of the Omega class glutathione transferases. J Biol Chem 275:24798–24806

Board PG (2011) The omega-class glutathione transferases: structure, function, and genetics. Drug Metab Rev 43:226–235

Boldyrev AA, Yuneva MO, Sorokina EV, Kramarenko GG, Fedorova TN, Konovalova GG, Lankin VZ (2001) Antioxidant systems in tissues of senescence accelerated mice. Biochemistry (Mosc) 66:1157–1163

Burmeister C, Luersen K, Heinick A, Hussein A, Domagalski M, Walter RD, Liebau E (2008) Oxidative stress in *Caenorhabditis elegans*: protective effects of the Omega class glutathione transferase (GSTO-1). FASEB J 22:343–354

Carlezon WA Jr, Duman RS, Nestler EJ (2005) The many faces of CREB. Trends Neurosci 28:436–445

Chowdhury UK, Zakharyan RA, Hernandez A, Avram MD, Kopplin MJ, Aposhian HV (2006) Glutathione-*S*-transferase-Omega [MMA(V) reductase] knockout mice: enzyme and arsenic species concentrations in tissues after arsenate administration. Toxicol Appl Pharmacol 216:446–457

Claudianos C, Ranson H, Johnson RM, Biswas S, Schuler MA, Berenbaum MR, Feyereisen R, Oakeshott JG (2006) A deficit of detoxification enzymes: pesticide sensitivity and environmental response in the honey bee. Insect Mol Biol 15:615–636

Cnubben NH, Rietjens IM, Wortelboer H, van Zanden J, van Bladeren PJ (2001) The interplay of glutathione-related processes in antioxidant defense. Environ Toxicol Pharmacol 10:141–152

Corona M, Robinson GE (2006) Genes of the antioxidant system of the honey bee: annotation and phylogeny. Insect Mol Biol 15:687–701

Ding YC, Hawkes N, Meredith J, Eggleston P, Hemingway J, Ranson H (2005) Characterization of the promoters of Epsilon glutathione transferases in the mosquito *Anopheles gambiae* and their response to oxidative stress. Biochem J 387:879–888

Dixon DP, Davis BG, Edwards R (2002) Functional divergence in the glutathione transferase superfamily in plants: identification of two classes with putative functions in redox homeostasis in *Arabidopsis thaliana*. J Biol Chem 277:30859–30869

Dulhunty A, Gage P, Curtis S, Chelvanayagam G, Board P (2001) The glutathione transferase structural family includes a nuclear chloride channel and a ryanodine receptor calcium release channel modulator. J Biol Chem 276:3319–3323

Enayati AA, Ranson H, Hemingway J (2005) Insect glutathione transferases and insecticide resistance. Insect Mol Biol 14:3–8

Ericsson A, Kotarsky K, Svensson M, Sigvardsson M, Agace W (2006) Functional characterization of the CCL25 promoter in small intestinal epithelial cells suggests a regulatory role for Caudal-Related Homeobox (Cdx) transcription factors. J Immunol 176:3642–3651

Frei B, England L, Ames BN (1989) Ascorbate is an outstanding antioxidant in human blood plasma. Proc Natl Acad Sci USA 86:6377–6381

Garcera A, Barreto L, Piedrafita L, Tamarit J, Herrero E (2006) *Saccharomyces cerevisiae* cells have three Omega class glutathione *S*-transferases acting as 1-Cys thiol transferases. Biochem J 398:187–196

Gilbert MD, Wilkinson CF (1975) An inhibitor of microsomal oxidation from gut tissues of the honey bee (*Apis mellifera*). Comp Biochem Physiol B 50:613–619

Habig WH, Pabst MJ, Jakoby WB (1974) Glutathione *S*-transferases. The first enzymatic step in mercapturic acid formation. J Biol Chem 249:7130–7139

Hayes JD, Flanagan JU, Jowsey IR (2005) Glutathione transferases. Ann Rev Pharmacol Toxicol 45:51–88

Huang YF, Xu ZB, Lin XY, Feng QL, Zheng SC (2011) Structure and expression of glutathione *S*-transferase genes from the midgut of the Common cutworm, *Spodoptera litura* (Noctuidae) and their response to xenobiotic compounds and bacteria. J Insect Physiol 57:1033–1044

Ishida M, Mitsui T, Yamakawa K, Sugiyama N, Takahashi W, Shimura H, Endo T, Kobayashi T, Arita J (2007) Involvement of cAMP response element-binding protein in the regulation of cell proliferation and the prolactin promoter of lactotrophs in primary culture. Am J Physiol Endocrinol Metab 293:E1529–E1537

Kampkötter A, Volkmann TE, de Castro SH, Leiers B, Klotz LO, Johnson TE, Link CD, Henkle-Duhrsen K (2003) Functional analysis of the glutathione *S*-transferase 3 from *Onchocerca volvulus* (Ov-GST-3): a parasite GST confers increased resistance to oxidative stress in *Caenorhabditis elegan*s. J Mol Biol 325:25–37

Ketterman AJ, Saisawang C, Wongsantichon J (2011) Insect glutathione transferases. Drug Metab Rev 43:253–265

Kim K, Kim SH, Kim J, Kim H, Yim J (2012) Glutathione *S*-transferase Omega 1 activity is sufficient to suppress neurodegeneration in a *Drosophila* model of Parkinson disease. J Biol Chem 287:6628–6641

Krishnan N, Sehnal F (2006) Compartmentalization of oxidative stress and antioxidant defense in the larval gut of *Spodoptera littoralis*. Arch Insect Biochem Physiol 63:1–10

Kottuparambil S, Shinb W, Browne MT, Han T (2012) UV-B affects photosynthesis, ROS production and motility of the freshwater flagellate, *Euglena agilis* Carter. Aquat Toxicol 122–123:206–213

Laliberte RE, Perregaux DG, Hoth LR, Rosner PJ, Jordan CK, Peese KM, Eggler JF, Dombroski MA, Geoghegan KF, Gabel CA (2003) Glutathione *S*-transferase Omega 1–1 is a target of cytokine release inhibitory drugs and may be responsible for their effect on interleukin-1β posttranslational processing. J Biol Chem 278:16567–16578

Livak KJ, Schmittgen TD (2001) Analysis of relative gene expression data using real-time quantitative PCR and the 2-(Delta Delta C (T)) method. Methods 25:402–408

Li HM, Buczkowski G, Mittapalli O, Xie J, Wu J, Westerman R, Schemerhorn BJ, Murdock LL, Pittendrigh BR (2008) Transcriptomic profiles of *Drosophila melanogaster* third instar larval midgut and responses to oxidative stress. Insect Mol Biol 17:325–339

Li X, Zhang X, Zhang J, Zhang X, Starkey SR, Zhu KY (2009) Identification and characterization of eleven glutathione *S*-transferase genes from the aquatic midge *Chironomus tentans* (Diptera: *Chironomidae*). Insect Biochem Mol Biol 39:745–754

Li YJ, Oliveira SA, Xu P, Martin ER, Stenger JE, Scherzer CR, Hauser MA, Scott WK, Small GW, Nance MA, Watts RL, Hubble JP, Koller WC, Pahwa R, Stern MB, Hiner BC, Jankovic J, Goetz CG, Mastaglia F, Middleton LT, Roses AD, Saunders AM, Schmechel DE, Gullans SR, Haines JL, Gilbert JR, Vance JM, Pericak-Vance MA, Hulette C, Welsh-Bohmer KA (2003) Glutathione *S*-transferase Omega-1 modifies age-at-onset of Alzheimer disease and Parkinson disease. Hum Mol Genet 12:3259–3267

Lourenco AP, Mackert A, Cristino AS, Simoes ZLP (2008) Validation of reference genes for gene expression studies in the honey bee, *Apis mellifera*, by quantitative real-time RT-PCR. Apidologie 39:372–385

Lumjuan N, McCarroll L, Prapanthadara L, Hemingway J, Ranson H (2005) Elevated activity of an Epsilon class glutathione transferase confers DDT resistance in the dengue vector, *Aedes aegypti*. Insect Biochem Mol Biol 35:861–871

Lushchak VI (2011) Environmentally induced oxidative stress in aquatic animals. Aquat Toxicol 101:13–30

Mahmoud KZ, Edens FW (2003) Influence of selenium sources on age-related and mild heat stress-related changes of blood and liver glutathione redox cycle in broiler chicken (*Gallus domesticus*). Comp Biochem Physiol B Biochem Mol Biol 136:921–934

Meng F, Kang M, Liu L, Luo L, Xu B, Guo X (2011) Characterization of the TAK1 gene in *Apis cerana cerana* (AccTAK1) and its involvement in the regulation of tissue-specific development. BMB Rep 44:187–192

Meng F, Zhang L, Kang M, Guo X, Xu B (2010) Molecular characterization, immunohistochemical localization and expression of a ribosomal protein L17 gene from *Apis cerana cerana*. Arch Insect Biochem Physiol 75:121–138

Michelette ERF, Soares AEE (1993) Characterization of preimaginal developmental stages in Africanized honey bee workers (*Apis mellifera* L). Apidologie 24:431–440

Ortelli F, Rossiter LC, Vontas J, Ranson H, Hemingway J (2003) Heterologous expression of four glutathione transferase genes genetically linked to a major insecticide-resistance locus from the malaria vector *Anopheles gambiae*. Biochem J 373:957–963

Poli G, Leonarduzzi G, Biasi F, Chiarpotto E (2004) Oxidative stress and cell signaling. Curr Med Chem 11:1163–1182

Rice ME (2000) Ascorbate regulation and its neuroprotective role in the brain. Trends Neurosci 23:209–216

Rival T, Soustelle L, Strambi C, Besson MT, Iche M, Birman S (2004) Decreasing glutamate buffering capacity triggers oxidative stress and neuropil degeneration in *Drosophila* brain. Curr Biol 14:599–605

Rørth P (1994) Specification of C/EBP function during *Drosophila* development by the bZIP basic region. Science 266:1878–1881

Rouimi P, Anglade P, Benzekri A, Costet P, Debrauwer L, Pineau T, Tulliez J (2001) Purification and characterization of a glutathione *S*-transferase Omega in pig: evidence for two distinct organ-specific transcripts. Biochem J 358:257–262

Scharlaken B, de Graaf DC, Goossens K, Brunain M, Peelman LJ, Jacobs FJ (2008) Reference gene selection for insect expression studies using quantitative real-time PCR: The honeybee, *Apis mellifera*, head after a bacterial challenge. J Insect Sci 8:1–10

Singh SP, Coronella JA, Benes H, Cochrane BJ, Zimniak P (2001) Catalytic function of *Drosophila melanogaster* glutathione *S*-transferase DmGSTS1-1 (GST-2) in conjugation of lipid peroxidation end products. Eur J Biochem 268:2912–2923

Stanojević D, Hoey T, Levine M (1989) Sequence specific DNA-binding activities of the gap proteins encoded by hunchback and Krüppel in *Drosophila*. Nature 341:331–335

Valko M, Izakovic M, Mazur M, Rhodes CJ, Telser J (2004) Role of oxygen radicals in DNA damage and cancer incidence. Mol Cell Biochem 266:37–56

Walters KB, Grant P, Johnson DL (2009) Evolution of the GST Omega gene family in 12 *Drosophila* species. J Hered 100:742–753

Wan Q, Whang I, Lee JS, Lee J (2009) Novel Omega glutathione *S*-transferases in disk abalone: characterization and protective roles against environmental stress. Comp Biochem Physiol C Toxicol Pharmacol 150:558–568

Wells WW, Xu DP, Washburn MP (1995) Glutathione: dehydroascorbate oxidoreductases. Methods Enzymol 252:30–38

Xun L, Belchik SM, Xun R, Huang Y, Zhou H, Sanchez E, Kang C, Board PG (2010) *S*-glutathionyl-(chloro)hydroquinone reductases: a novel class of glutathione transferases. Biochem J 428:419–427

Yamamoto K, Zhang P, Miake F, Kashige N, Aso Y, Banno Y, Fujii H (2005) Cloning, expression and characterization of theta-class glutathione *S*-transferase from the silkworm, *Bombyx mori*. Comp Biochem Physiol B Biochem Mol Biol 141:340–346

Yamamoto K, Teshiba S, Shigeoka Y, Aso Y, Banno Y, Fujiki T, Katakura Y (2011) Characterization of an Omega-class glutathione *S*-transferase in the stress response of the silkmoth. Insect Mol Biol 20:379–386

Yin S, Li X, Meng Y, Finley RL Jr, Sakr W, Yang H, Reddy N, Sheng S (2005) Tumor-suppressive maspin regulates cell response to oxidative stress by direct interaction with glutathione *S*-transferase. J Biol Chem 280:34985–34996

Yu F, Kang M, Meng F, Guo X, Xu B (2011) Molecular cloning and characterization of a thioredoxin peroxidase gene from *Apis cerana cerana*. Insect Mol Biol 20:367–378

Zhou H, Brock J, Liu D, Board PG, Oakley AJ (2012) Structural insights into the dehydroascorbate reductase activity of human Omega-class glutathione transferases. J Mol Biol 420: 190–203